

# Fabrication of PLGA nanoparticles using combination of PCL PVA PEG copolymer as surfactant: In vitro characterization and cytotoxicity study

Shashi Ranjan<sup>1</sup>, Subas Chandra Dinda<sup>2</sup>, Anurag Verma<sup>1</sup>

<sup>1</sup> Department of Pharmaceutics, College of Pharmacy, Teerthanker Mahaveer University, Moradabad, Uttar Pradesh, India

<sup>2</sup> The Neotia University, School of Pharmacy, Sarisa, West Bengal, India

ABSTRACT

**Background:** The present study aimed to fabricate Poly Lactic acid Co-Glycolic Acid (PLGA) nanoparticles loaded with resveratrol using a novel graft copolymer surfactant named soluplus®.

**Materials and Methods:** The PLGA nanoparticles were prepared in the present study using polyvinyl caprolactam, polyvinyl acetate polyethylene glycol amphiphilic graft copolymer named soluplus® as surfactant through double emulsification and single emulsification-solvent evaporation method. The formulations were prepared successfully to encapsulate the drug resveratrol, and then evaluated for their particle size, polydispersity index, zeta potential, drug loading and the degree of entrapment of the drug. Using a scanning electron microscope, the nanoparticles' morphology was investigated. In vitro drug release was evaluated, and the release pattern was evaluated using mathematical pharmacokinetic modelling. A comparative cytotoxicity study between free drug and prepared nanoparticles using MTT assay was carried out for cell viability evaluation. Uptake and internalization of nanoparticles were also studied using confocal fluorescence microscopy.

**Results and Discussion:** The outcomes showed that PLGA nanoparticles may be successfully fabricated utilising soluplus as a polymer surfactant. The drug, polymer and the all the excipients were found to be compatible and did not indicate any interaction. The results also indicated the prepared nanoparticles Surfactants-2 (SF2) as suitable resveratrol delivery vehicle in terms of the compliant particle size (344.6 nm ± 6.63 nm), polydispersity index (0.962), zeta potential (-18.5% ± 1.21%), drug loading (18.94% ± 0.27%), the entrapment efficiency (39.62% ± 0.17%) and drug release (75.13% ± 0.17%). The shape and surface morphology of the formulated nanoparticles were found to be spherical and smooth. Cytotoxicity study also demonstrated significant reduction of cell viability by the nanoparticle compared to free resveratrol. The highest cytotoxicity of SF2 against Michigan Cancer Foundation-7 (MCF7) cell was found in 2000 nM concentration with 3.03% ± 0.05% of cell viability. It was found that the percentage of growth inhibition was increasing with increasing concentration of SF2 and Inhibitory Concentration (IC)<sub>50</sub> value of this assay was 108.94 µg/ml.

**Conclusion:** It has been found that the resveratrol loaded PLGA nanoparticles were successfully formulated and found to perform better in terms of efficacy and cytotoxicity.

**Keywords:** resveratrol, PLGA, nanoparticles, soluplus®, anticancer, cytotoxicity

## Address for correspondence:

Shashi Ranjan,  
Department of Pharmaceutics, College of Pharmacy, Teerthanker Mahaveer University, Moradabad, Uttar Pradesh, India Email: ranjanshashi20@gmail.com

**Word count:** 7181 **Tables:** 05 **Figures:** 08 **References:** 63

**Received:** 10 April, 2024, Manuscript No. OAR-24-131948

**Editor Assigned:** 12 April, 2024, Pre-QC No. OAR-24-131948(PQ)

**Reviewed:** 25 April, 2024, QC No. OAR-24-131948(Q)

**Revised:** 02 May, 2024, Manuscript No. OAR-24-131948(R)

**Published:** 10 May, 2024, Invoice No. J-131948

## INTRODUCTION

In biomedical research, particularly for applications involving drug delivery, Polymeric Nanoparticles (PNPs) preparation techniques are of great interest. PNPs have several goals in drug delivery applications, including controlled drug release, biocompatibility with tissues and cells, higher intracellular uptake than free drugs, improved stability of active ingredients, and the ability to target particular tissues [1-3]. The PNPs size is an important consideration in the design of these systems; they should be large enough to slow down incorporation into blood vessels while still being small enough to avoid immune system destruction [4]. To satisfy each of these requirements, the PNP preparation methods should be examined and modified for each active substance. Additionally, in order to produce reproducible large batches, it is crucial to study the PNP preparation methods [5, 6]. The most popular polymer used in the production of PNP is Poly Lactic acid Co-Glycolic Acid (PLGA). Because of its biodegradability and low systemic toxicity, PLGA is successfully used in the research of drug delivery systems and has received FDA approval for use in medical applications [7-10].

Several techniques, including emulsification evaporation, nanoprecipitation or solvent displacement, solvent diffusion, and phase-inversion, can be used to formulate PNP using PLGA into, with sizes ranging from 10 nm to 1000 nm [11]. When encapsulating hydrophobic compounds, two of the most commonly used techniques are the emulsification-solvent evaporation technique and the nanoprecipitation technique [12]. Solution for the efficient formulation of hydrophobic drugs has been emerged with the use of nano size polymeric particles. In addition to their rapid dissolution rate, these systems are highly regarded for their high bioavailability after oral administration, because of enhanced absorption of the medication. Their capacity to solve issues related to poorly lipid- and water-soluble medicines is unique because to their simplicity and advantages over alternative delivery systems. Nanoscale drug particles were produced as colloidal dispersions using an appropriate technique and stabilizer [13-16]. In breast cancer models, resveratrol is shown to suppress the expression of cyclin D1 and E as well as cyclin-dependent kinases 2 and 4 along with Insulin-like Growth Factor-1 (IGF-1) by minimizing the expression of cell cycle regulatory proteins [17-20]. As a result of the low solubility and instability of resveratrol, its activity is limited, as it is not readily bioavailable and is readily metabolized [21-24]. A very scant amount of literature exists on the preparation of formulations of

resveratrol that will increase its efficacy and overcome its related issues. In fact, targeting natural bioactive is one of the greatest challenges [25-27]. It was the purpose of our study to explore the use of an amphiphilic polymeric, soluplus®, in the stabilization of nano formulations which were designed and evaluated to be effective for the administration of resveratrol, a poorly soluble model drug used in this study. Especially manufactured by BASF for formulating poorly soluble drugs, Soluplus® is a polyvinyl caprolactam-polyvinyl acetate-polyethylene glycol amphiphilic graft copolymer. Since it is bifunctional, it is expected to function as an effective matrix for dissolving drugs in water. In the fourth generation of solid solutions, soluplus® is a new polymer specifically designed to enhance dissolution. Drugs that are poorly soluble can be made more soluble and bioavailable by soluplus®. The objective of this study to determine whether soluplus® can be used to synthesize nanoparticles as a surfactant to enhance their wetting characteristics and decrease agglomeration, as well as to evaluate the drug loading and entrapment efficiency, particle size, polydispersity index, zeta potential and surface morphology of the prepared drug loaded nanoparticles.

## MATERIAL AND METHOD

### Drug and chemicals

The PLGA (85:15,  $M_w$  200,000) was purchased from Sigma Aldrich, as it is a commercially available product. A gift sample of Resveratrol was provided by Zorion Drugs and Herbs Pvt. Ltd, Ambala. As for soluplus®, a graft co-polymer of polyvinyl caprolactam-polyvinyl acetate-polyethylene glycol, it was provided as gift sample from BASF (USA). For the purpose analytical grade chemicals were used.

### Drug excipient compatibility

It is possible for the drug degradation to occur as a result of the interaction between the drug and the excipient. Compatibility of the excipients is crucial for the formation of stable and efficient dosage forms. With FTIR spectroscopy, potential medication interactions were investigated.

### FTIR (Fourier-Transform Infrared spectroscopy)

The FTIR spectra for a physical blend of pure drug and excipients was obtained by using FTIR spectrophotometer (Bruker Instrument, Germany) and analysed the obtained IR spectra to ascertain the interaction between the drug and the prepared lyophilized formulation by comparing their FTIR spectra at wavelengths between 400  $\text{cm}^{-1}$  and 4000  $\text{cm}^{-1}$ .

### Formulation of nanoparticles

#### Soluplus® as a stabilizer in Double Emulsification and Solvent Evaporation (DESE) method:

Resveratrol-loaded PLGA polymer-based nanoparticles were produced by employing soluplus® as a surfactant in different amounts and concentrations. 2.5 milliliters of dichloromethane were used to dissolve 10 mg of resveratrol. In the medication and dichloromethane solution, about 20 mg of polymers PLGA were dissolved (drug-polymer ratio: 1:2). 2.5 ml of 1.5% w/v Soluplus® was homogenized dropwise for 20 minute–30 minute at 3,000 rpm in order to produce a rich, creamy emulsion. The creamy foam consistency of the main emulsion was homogenised with 25 ml of 0.5% w/v Soluplus® for 20 minutes–30 minutes at 18,000

rpm to create a secondary emulsion. The secondary emulsion was sonicated for 45 minutes, and then the organic solvents were removed by stirring it with a magnetic stirrer overnight. The larger particles that developed in the double emulsion were disposed of after five minutes of centrifugation at 5,000 rpm. The supernatant was centrifuged once more for 30 minutes at 7,000 rpm. It was then rinsed three times with distilled water and freeze-dried to produce nanoparticles. The code designation assigned to this initial formulation was Surfactants-1 (SF1). It was made using Soluplus® in primary and secondary emulsions at the same concentrations (1.5% w/v and 0.5% w/v), but in secondary emulsions, the volume was increased from 5 ml to 50 ml [28, 29].

#### Single Emulsification and Solvent Evaporation (SESE) using soluplus® as stabilizer:

A quantity of 2.5 ml of dichloromethane was used to dissolve 10 mg of resveratrol. The drug to polymer ratio is 1:2 with the addition of 20 mg of polymer. A 10 minute to 15 minute homogenization at 15,000 rpm after dropwise adding the drug-polymer solution to 50 cc, 2.5% w/v soluplus® resulted in an emulsion. The development of stable emulsions is indicated by creamy emulsions. Dichloromethane was extracted using a 45 minute sonication and 12 hours-14 hours of gentle magnetic stirring. The solution was repeatedly rinsed three times with distilled water after centrifuging it for 30 minutes at 15,000 rpm to remove the surfactant, and the nanoparticles were freeze-dried. Surfactants-3 (SF3) was the code designation for the formulation. Furthermore, utilising 1.5% w/v soluplus®, 50 ml of formulation Surfactants-4 (SF4) was made [30, 31].

### Characterization of PLGA nanoparticles

#### Percentage yield, drug loading and entrapment efficiency:

The following formula was used to determine the yield, or percentage, of nanoparticle formulations made using both the DESE and SESE procedures [14]:

$$\text{Percentage Yield} = \frac{\text{Weight (nanoparticles obtained)}}{\text{Weight (drug and polymer used for nanoparticles preparation)}} \times 100$$

The entrapment and loading efficiency of the nanoparticles were measured using a centrifuge tube loaded with dichloromethane and 2 mg of Resveratrol-laden nanoparticles. In a shaker incubator, the mixture was continuously shaken for three to four hours at 37°C. Using centrifugation, the continuous and dispersed phases were separated. Using a UV-Visible spectrophotometer set to 475 nm in wavelength, the concentration of the collected supernatant was evaluated in order to ascertain the drug release. We employed the following formulas to get the percentages of drug loading efficiency and entrapment efficiency [30, 31]:

$$\text{Drug loading efficiency (\%)} = \frac{\text{Drug Amount present in nanoparticles}}{\text{Drug Amount loaded nanoparticles}} \times 100$$

$$\text{Entrapment efficiency (\%)} = \frac{\text{Drug Amount present in nanoparticles}}{\text{Initial Drug Amount added}} \times 100$$

#### Particle size and zeta potential:

Using solid-state lasers, a Malvern Nano ZS90 outfitted with a Dynamic Light Scattering (DLS) system was used to measure the sizes and distributions of nanoparticles. Prior to

measurement, an appropriate quantity of desiccated nanoparticles was dissolved in double-distilled water and subjected to a reasonable duration of sonication. Next, the size distribution of the homogeneous suspension, the polydispersity index, and the average hydrodynamic particle size were computed. The Malvern NANO ZS90 was also used to detect Zeta Potential (ZP). ZP provides information on the particle surface charge and long-term stability of dried nanoparticles from every formulation. Before measurement, these nanoparticles were suspended in double-distilled water and subjected to a reasonable amount of sonication.

#### Scanning Electron Microscopy (SEM):

Using a scanning electron microscope, the formed nanoparticles' shape and surface morphology were investigated (Hitachi SEM, S-3600 N). To obtain an adequate sample of nanoparticles, a sample was placed onto metal stubs using double-sided carbon tape and broken with a razor blade. After the samples were gold-sputter coated, their morphology was investigated in an argon atmosphere using a secondary electron emissive SEM.

#### In vitro drug release study:

To investigate drug release from formed nanoparticles, a phosphate buffer with a pH of 7.4 was utilised. Eppendorf tubes containing 5 mg of freeze-dried nanoparticles were filled with 2 ml of phosphate buffer and incubated at 37°C for drug release investigations. Following 0, 1 hour, 3 hours, 6 hours, 9 hours, 12 hours, 24 hours, 36 hours, and 48 hours of shaking at 120 rotations per minute, the samples were centrifuged. After that, 0.5 ml of the supernatant was taken and its concentrations were evaluated using a UV-visible spectrophotometer set to 475 nm in order to determine the drug release study's rate. The buffer with the same pH was used in place of the withdrawal volume.

#### In vitro drug release kinetic study:

It is crucial to investigate the method by which medications are released from nanoparticles in order to comprehend their pharmacokinetic properties. Based on kinetic equations, such as zero-order, first-order, etc., in vitro drug release data were analysed, and graphs were created using these equations. based on charts that are linear. To find  $R^2$  and  $k$ , a regression analysis was conducted [32, 33].

#### Cytotoxicity assay using MCF7 cells:

Formazan was used to measure the cytotoxicity of blank and resveratrol-encapsulated nanoparticles on MCF-7 breast cancer cells by reducing 3-(4, 5-dimethylthiazol-2-yl)-2, 5-diphenyl tetrazolium bromide (MTT, Sigma) [34-37]. In short, MCF7 (mice breast cancer cell line) cells were sown in a 5000/well flat-bottom 96-well culture plate. After that, it was incubated for 24 hours with various PLGA-NP concentrations (0 nm-2000 nm Resveratrol equivalent) and drug free. After the medium was withdrawn, the cells were incubated with MTT solution (5 mg/ml in PBS) at 37°C. Untreated cells were used as the control group. After three hours of incubation, the supernatant was collected, and the cells were then treated with 100  $\mu$ L of DMSO to dissolve the dark blue formazan crystals. The absorbance was then measured at 570 nm using an ELISA reader.

#### Cellular uptake of nanoparticles by confocal fluorescence microscopy:

The MCF7 cells' absorption of PLGA-NPs was evaluated

qualitatively between 38 and 43. Fluorescein Isothiocyanate (FITC) labeled PLGA NPs were employed. Using fluorescence microscopy, the presence of NPs in breast cancer cells (MCF7) was investigated. In short, MCF-7 cells were seeded with Dulbecco's Modified Eagle's Medium (DMEM) onto a 24-well plate, with 10,000 cells per well, following pre-treatment. DAPI, or 4', 6-diamidino-2-phenylindole, was employed to label the cell nucleus. To summarise, the cells were trypsinized, then washed with PBS and fixed for 10 minutes with 3.7% formaldehyde. The cells were washed, then treated for five minutes with 0.2% Triton X-100, and lastly for five minutes with an appropriate volume of DAPI labelling solution (1:5000 DAPI in PBS). Following PBS washing, fluorescent microscopy was used to analyse the cells [38-43].

## RESULTS

### Drug-excipient compatibility studies

The principal and distinguishing peaks of the medication and the excipients were preserved, as we have seen from the separate FTIR spectra of PLGA, Resveratrol, and Soluplus<sup>®</sup>, as well as by comparing them to the FTIR spectrum obtained for the physical mixture of PLGA-resveratrol-soluplus<sup>®</sup> (Figure 1). Consequently, the excipients did not exhibit any incompatibility, indicating that they were likewise totally stable. The FTIR spectra of resveratrol shows a significant olefinic band at 965  $\text{cm}^{-1}$  and 3293  $\text{cm}^{-1}$ , which is caused by OH stretching vibration. The band at 1383  $\text{cm}^{-1}$  and 1586  $\text{cm}^{-1}$  shows that resveratrol demonstrates CO stretching. In the FTIR examination of the PLGA polymer, peaks at wave numbers 692  $\text{cm}^{-1}$ , 1008  $\text{cm}^{-1}$ , 1370  $\text{cm}^{-1}$ , 1627  $\text{cm}^{-1}$ , 1960  $\text{cm}^{-1}$ , and 2257  $\text{cm}^{-1}$  were plainly apparent. Furthermore, the peaks in both the PLGA and nanoparticles at 2441  $\text{cm}^{-1}$  and 3406  $\text{cm}^{-1}$  verify that PLGA is present in the formulation. The OH stretching band shifts to a higher wave number due to the hydrogen bonding between the hydroxyl groups in resveratrol and the carbonyl groups in PLGA.

### Nanoparticle preparation

In this work, resveratrol-containing nanoparticles were produced using two different methods. Table 1 shows two evaporation methods: Single Emulsion Solvent Evaporation (SESE) and Double Emulsion Solvent Evaporation (DESE). It was discovered that formulations with the necessary size, encapsulation, and surface qualities could be created using either of the approaches. The full emulsification of the organic and aqueous phases is the most important component of the emulsion process. PVA is a regularly used stabiliser, although several stabilisers are employed as well. In this investigation, Soluplus<sup>®</sup> was utilised in place of PVA. Table 2 demonstrates that both approaches provide enough particles, suggesting an improved formulation.

### Characterization of nanoparticles Scanning Electron Microscopy (SEM) and particle size analysis

SEM pictures of NPs with spherical forms and smooth surfaces may be seen in figure 2 below. Table 2, demonstrates that the resveratrol-loaded particles were uniformly distributed and submicron in size under the experimental conditions based on their polydispersity index results.

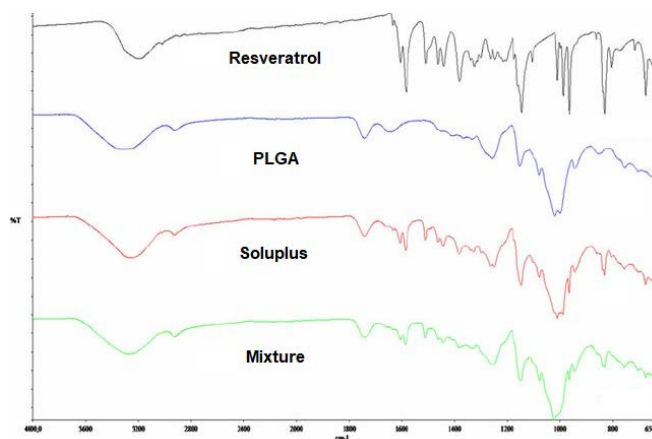


Fig. 1. FTIR spectrum of resveratrol, plga, soluplus® and physical mixture

Tab. 1. Nanoparticles compositions (SF1-SF4) and percentage yield of the nanoparticles

Formulation code		SF1	SF2	SF3	SF4
Resveratrol (mg)		10	10	10	10
Polymer used		PLGA 85:15	PLGA 85:15	PLGA 85:15	PLGA 85:15
Amount of polymer (mg)		20	20	20	20
Method used		DESE	DESE	SESE	SESE
Stabilizer soluplus® (% w/v) and volume (ml)	Primary	1.5 and 2.5	1.5 and 5	2.5 and 50	1.5 and 50
	Secondary	0.5 and 25	0.5 and 50	---	---
Percentage yield		73.52	73.78	72.78	74.87

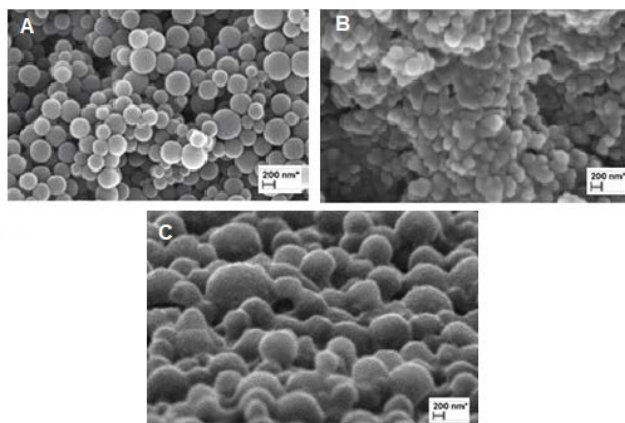


Fig. 2. SEM images of prepared PLGA nanoparticles (A- SF2, B- SF3 and C- SF4)

The spherical nature of polymeric nanoparticles was demonstrated by SEM pictures. The lyophilized resveratrol-loaded polymeric nanoparticles in the optimised formulation had a cumulative percentage drug release of  $75.13\% \pm 0.17\%$  after 48 hours, which was higher than that of the prior formulations. The efficacy, safety, and therapeutic effect of chemicals can be negatively impacted by a variety of circumstances, such as insufficient drug delivery to the intended tissues or unfavourable side effects including extreme toxicity in healthy tissues. When a medication is enclosed in nanocarriers with specific and foreseeable characteristics, the medication's bioavailability is increased and its adverse effects are decreased. Based on their physicochemical properties, the size distribution of particles within nanocarriers influences their propensity to collect in target tissues. Therefore, in order to create safe, stable, and effective nanocarriers, homogeneous (monodisperse) populations of nanocarriers of a particular size must be prepared. However, without considering the makeup of the nanocarriers and the type of solvents and cosolvents used to create them, con-

trolling the distribution of particle sizes is difficult [44, 45].

### Polydispersity Index (PDI) and zeta potential (mV)

They need to be defined in order to guarantee that both in vitro and in vivo applications can be carried out on the polydispersity index, or PDI. An essential variable in characterising the particle size distribution is the Polydispersity Index (PDI). This index lacks a dimension and is scaled to only be seen in standards with large monodisperse distributions, which often have values less than 0.05. Because of its wide particle size distribution, an example with a particle size distribution greater than 0.7 is unlikely to be further improved. It is possible to identify size and PDI parameters (0.05-0.7) using a range of size distribution algorithms when the data falls between these two extreme values of PDI [46]. In terms of particle size, PDI, and zeta potential, the Surfactants-2 (SF2) formulation outperformed all other nanoformulations by a wide margin. To ascertain the surface charge of

nanoparticles loaded with resveratrol, Zeta Potential (ZP) was assessed. The zeta potential of nanoparticles influences both their pharmacokinetics and biodistribution outside of the physiological milieu. Negatively charged nanoemulsions are easily absorbed by the reticuloendothelial system and are excreted more quickly than neutrally or positively charged nanoemulsion. Moreover, the kind

of binding that occurs between medications and nanoparticles as well as the zeta potential of the latter two influence drug loading efficiency and the rate at which pharmaceuticals can be reabsorbed from nanoparticles. Determining whether the medicine or active component is adsorbing on the surface of the nanoparticles or is encapsulated at the center can also be helpful.

**Tab. 2.** Characteristics of resveratrol loaded polymeric nanoparticles using Soluplus® as surfactant

Formulation Code	Particle Size (nm)	Polydispersity Index (PDI)	Zeta Potential (mv)	Drug Loading (%)	Entrapment Efficiency (%)
				(Mean ± SD)	
SF1	568.7 ± 9.87	0.716	-23.2 ± 1.08	17.90% ± 0.16%	36.78% ± 0.16%
SF2	344.6 ± 6.63	0.962	-18.5 ± 1.21	18.94% ± 0.27%	39.62% ± 0.17%
SF3	526.2 ± 12.36	0.917	-18.4 ± 1.33	18.12% ± 0.13%	35.18% ± 0.14%
SF4	571.3 ± 11.97	0.977	-16.8 ± 1.09	18.21% ± 0.26%	36.43% ± 0.21%

It has been shown that negatively charged nanoparticles are more slowly eliminated from the system and remain in the bloodstream longer than positively charged nanoparticles following intravenous

delivery. Studies also show that nanoparticles' cationic charge, or negative zeta potential, increases their cytotoxicity (Figure 3).

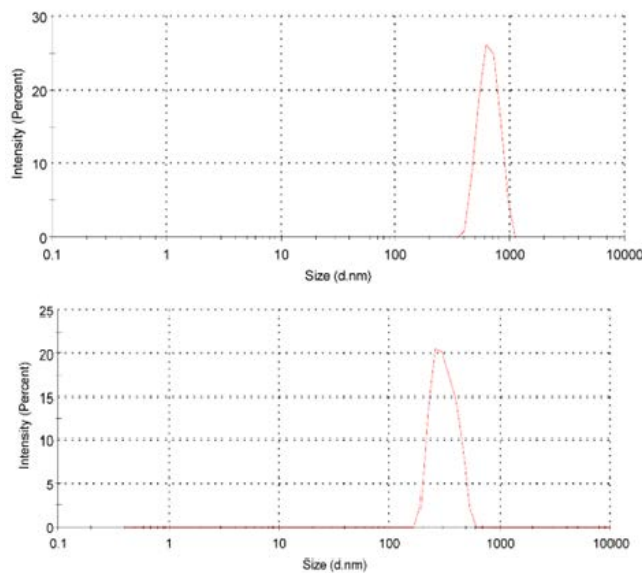


**Fig. 3.** The SF1 and SF2 particle size distribution curves

The oppositely charged cell membrane may become unstable and even damaged as a result of the interaction between nanoparticles and the membrane [47]. Additionally, it was discovered that the formulations had negative, demonstrating the stability of the polymeric nanoparticles. When used as a surface-active agent,

Soluplus®-prepared PLGA nanoparticles show encouraging zeta potential profiles for encasing hydrophobic medications like resveratrol. Considering all of the results, Soluplus® was shown to be a somewhat mediocre (in comparison to PVA) option when creating PLGA nanoparticles in this investigation (Figure 4 and 5).

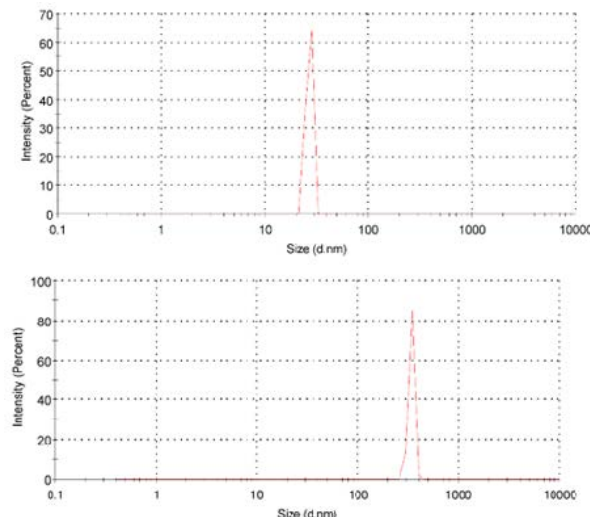


**Fig. 4.** The SF3 and SF4 particle size distribution curves

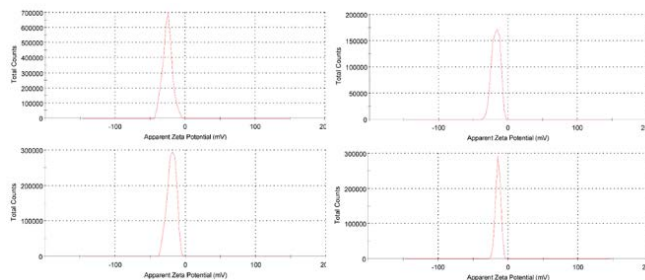


Fig. 5. SF1, SF2, SF3, and SF4's zeta potential

### Entrapment efficiency and drug loading

The percent entrapment efficiency and percentage drug loading of the formulations were observed to vary, with values ranging from 17.90% ± 0.16% to 18.94% ± 0.27% and from 35.18% ± 0.14% to 39.62% ± 0.17%, respectively. The drug polymer ratio and stabiliser concentration were shown to be significantly influencing

both drug loading and entrapment efficiency, based on the values of these parameters. Metrics like drug-polymer ratio, homogenization rate, and stabiliser are important parameters that affect drug loading and entrapment effectiveness. Using PLGA polymer, it was discovered that drug loading was seven times more at a 1:1 drug to polymer ratio than at a 1:3 ratio (Figure 6) [48].

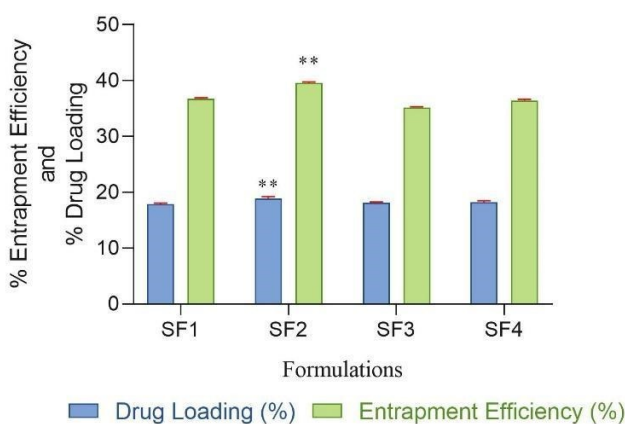


Fig. 6. Drug loading and entrapment efficiency of SF1–SF4

nanoformulations. SF2 proved to perform noticeably better than the other formulas (\*\*p<0.01)

### In vitro drug release and pharmacokinetic modeling of resveratrol loaded PLGA nanoparticles

The in vitro drug release ranges for all formulations were determined to be 18.82% ± 0.14% to 22.36% ± 0.23% at one hour. The release was discovered to be between 40.27% ± 0.11% and 47.97% ± 0.13% at the third hour. The acquired data also demonstrates that, as opposed to a dramatic explosion of release during the first three hours of the in vitro investigation, drug release

increases steadily after the third hour. This release pattern could be the result of PLGA degradation at first, followed by gradual diffusion up to 75.13% ± 0.17% after 48 hours. In comparison to other formulations, formulation (SF2) had the maximum drug release of 75.13% ± 0.17% at 48 hours. When the release kinetic pattern of these in vitro drug release data was examined, the R2 values indicated that there was zero order release kinetics after strong linearity in the Korsmeyer-Peppas plot (Figure 7 and Table 3).

Tab. 3. In vitro drug release data from PLGA nanoparticles

Time (hours)	Cumulative percentage drug release (Mean ± SD)			
	Surfactants-1 (SF1)	Surfactants-2 (SF2)	Surfactants-3 (SF3)	Surfactants-4 (SF4)
0	0	0	0	0
1	19.94% ± 0.09%	22.36% ± 0.23%	18.82% ± 0.14%	19.24% ± 0.15%
3	43.34% ± 0.06%	47.97% ± 0.13%	40.27% ± 0.11%	41.28% ± 0.19%
6	45.09% ± 0.1%	53.32% ± 0.08%	43.91% ± 0.15%	43.61% ± 0.11%
9	49.73% ± 0.09%	57.61% ± 0.1%	48.33% ± 0.13%	47.02% ± 0.08%
12	53.39% ± 0.16	59.75% ± 0.11%	50.96% ± 0.07%	50.13% ± 0.07%
24	58.56% ± 0.11%	64.75% ± 0.06%	55.41% ± 0.17%	53.2% ± 0.09%
36	64.65% ± 0.08%	70.51% ± 0.15%	60.44% ± 0.1%	57.35% ± 0.13%
48	68.94% ± 0.1%	75.13% ± 0.17%	64.09% ± 0.12%	61.02% ± 0.16%

The drug release from the polymeric formulations is confirmed by the kinetic modelling of the in vitro drug release data, which shows the release process based on the Korsmeyer-Peppas model. The drug releases eventually. Its release mechanism also follows Fickian diffusion, according to formulation SF2, as indicated by the n value of 0.148. For the drug release from the polymeric en-

capsulated system, the above finding clearly implies zero order release along with a diffusion process.

Table 4 below displays the various rate constants and release exponents that were computed from drug release research data using different kinetic models.

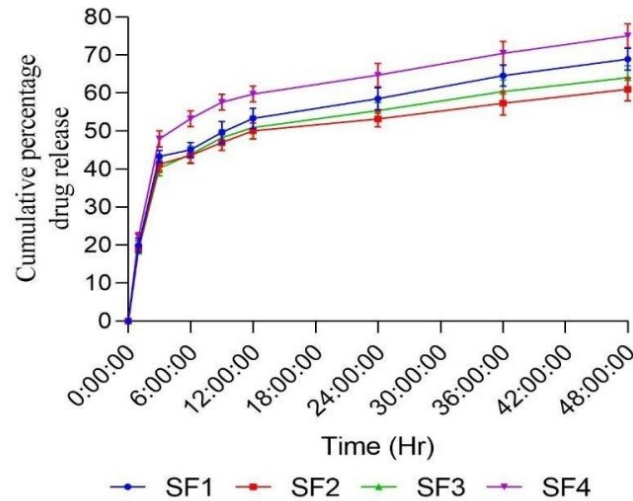


Fig. 7. Graph showing the cumulative percent drug released vs time profile

Tab. 4. In vitro drug release data with different kinetic models	Formulation Code	Zero Order Model	First Order Model	Higuchi Model	Hixon-Crowell Model	Korsmeyer-Peppas Model	
		$R^2_z$	$R^2_f$	$R^2_H$	$R^2_{HC}$	$R^2_{KP}$	n
	SF1	$0.984 \pm 0.0073$	$0.661 \pm 0.0052$	$0.838 \pm 0.0029$	$0.306 \pm 0.0043$	$0.976 \pm 0.0087$	$0.128 \pm 0.0017$
	SF2	$0.984 \pm 0.0075$	$0.598 \pm 0.0087$	$0.793 \pm 0.0082$	$0.288 \pm 0.0077$	$0.965 \pm 0.0076$	$0.119 \pm 0.0028$
	SF3	$0.963 \pm 0.0062$	$0.673 \pm 0.0053$	$0.823 \pm 0.0014$	$0.308 \pm 0.0017$	$0.989 \pm 0.0091$	$0.164 \pm 0.0053$
	SF4	$0.984 \pm 0.0021$	$0.672 \pm 0.0061$	$0.803 \pm 0.0014$	$0.302 \pm 0.0014$	$0.987 \pm 0.0096$	$0.168 \pm 0.0052$

### Cytotoxicity evaluation using MTT assay

A cytotoxicity research was conducted using SF2 against MCF7 cell lines at various doses in order to determine the IC<sub>50</sub> (50% growth inhibition) using the MTT test. Figure 8 presents the outcomes of various SF2 concentrations. When SF2 was compared to control and free drug, the MTT assay revealed a substantial impact on MCF7 cells in concentration ranges between 100 nM and 2000 nM. At 2000 nM concentration, SF2 exhibited the maximum cytotoxicity against MCF7 cells, maintaining  $3.03\% \pm$

0.05% of cell viability. It was discovered that as SF2 concentration increased, the percentage of growth inhibition increased as well. The assay's IC<sub>50</sub> value was 108 µg/ml. Using linear regression analysis in the Graph-Pad Prism software programme, the IC<sub>50</sub> values for the PLGA nanoparticles and free resveratrol in the MCF7 cells were also determined. The results indicate that the IC<sub>50</sub> values for PLGA nanoparticles and free resveratrol were 108.94 µg/mL and 231.52 µg/mL, respectively (Table 5).

Tab. 5. EC <sub>50</sub> values for the free resveratrol and the PLGA nanoparticles in the MCF7 cells	Sl. No.	Composition/Product	EC <sub>50</sub> (µg/mL)
	1	Free resveratrol	231.52 µg/mL
2	PLGA nanoparticles (Resveratrol loaded)	108.94 µg/mL	

**Fluorescent imaging microscopy: uptake of nanoparticles by the breast cancer cells (MCF7)**  
To investigate whether Resveratrol-encapsulated NPs were internalized into the breast cancer cell line MCF7, cellular uptake of FITC labeled PPF-NPs were analyzed by fluorescent imaging

microscopy. The Uptake of FITC labeled PLGA nanoparticles were also evaluated by fluorescent imaging microscopy (Figure 8). The results showed that FITC labelled PLGA nanoparticles were internalized into the MCF7 cells effectively.

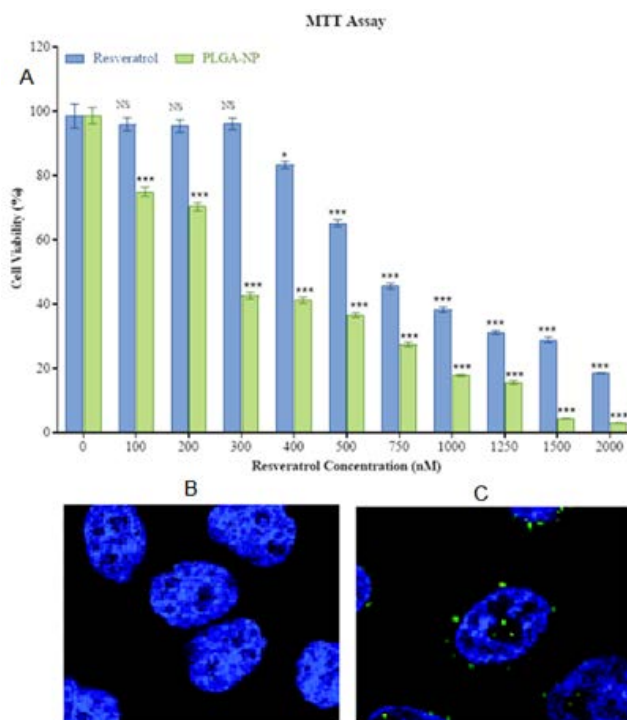


**Fig. 8.** Bioevaluation using cytotoxicity assessment of the PLGA nanoparticles **A.** Cytotoxicity as compared free drug **B.** Results of fluorescent imaging microscopy showing the internalization PLGA nanoparticles in control MCF7 cells and **C.** Results of fluorescent imaging microscopy showing the internalization PLGA nanoparticles into the MCF7 cells

## DISCUSSION

Poly(lactic-co-glycolic acid) (PLGA), a biodegradable polymer-based nanoparticle, is widely used to solve problems with drug insolubility, plasma circulation, and plasma concentration of different medicinal and active therapeutic components [49]. In addition to weakly soluble or lipophilic medications, these polymeric nanoparticles can target genes found in cancer tissues. Because tumour cells share physiological traits such as leaky vasculature and lack of a lymphatic system, they favour an effect known as the Enhanced Permeation and Retention (EPR) effect. Furthermore, because nanoparticles can enter cells and lessen P-glycoprotein-mediated cell efflux, they can slow the development of multiple drug resistance. However, developing a targeted, attractive, and active delivery system that can increase drug internalization at the cancer site is a difficult task [50, 51]. Polymeric nanoparticle-based drug delivery techniques are one of the fastest-growing areas of nanotechnology. Numerous medications, including biologic macromolecules, hydrophilic and hydrophobic small medicines, vaccinations, and oral and inhalation uses, may be delivered via nanoparticles. Additionally, these particles are very stable, very carrier-competent, and capable of incorporating both hydrophilic and hydrophobic materials [52, 53]. In the current work, resveratrol-loaded polymeric nanoparticles were produced using the double and single emulsion-solvent evaporation techniques. A stabiliser called soluplus® was employed. The synthesised polymeric nanoparticle formulations loaded with resveratrol were evaluated for their physicochemical properties. Based on characterization, a formulation was selected as the best formulation. Using Scanning Electron Microscopy (SEM), the optimised formulation's morphological characteristics were further examined. The spherical nature of polymeric nanostructures was demonstrated using SEM pictures. Compared to earlier formulations, the optimised formulation demonstrated a greater cumulative percentage drug re-

lease of lyophilized Resveratrol-loaded nanoparticles at 48 hours,  $75.130\% \pm 0.17\%$ . Based on in-vitro drug release kinetics studies,  $R^2$  values in the Korsmeyer-Peppas plot were shown to be more linear, and zero order kinetics followed. The drug release exponent (n value) was less than 0.5, according to the Korsmeyer-Peppas plot, suggesting "Fickian diffusion" of the drug from the matrix type nanoparticle formulation. In the end, the purpose of the study was accomplished by developing a controlled release mechanism nanoparticulate drug delivery system for resveratrol using Poly(lactic Acid) (PLGA). The method used in this work allowed for the rapid and reliable fabrication of a scaffold of nanoparticles with a homogeneous, spherical morphology. Several investigations that produced PLGA base nanoparticles reported similar results, which were then published in the literature [54-57]. As a result, it can be concluded that the formulation developed in this work holds potential for use as a long-term cancer therapeutic treatment for anticancer drug delivery [58, 59]. This work aimed to design and create a customised delivery system for resveratrol to improve its absorption by breast cancer cells and address related concerns. This work develops a novel drug delivery strategy by emulsifying PLGA nanoparticles with resveratrol. The hypothesis posits that the intravenous administration of Nanoparticles (NPs) will facilitate the sustained delivery of resveratrol to a particular tumour site while safeguarding it from fast breakdown [59, 60]. To specifically deliver resveratrol to tumours, nanoparticles containing the synthesised biodegradable target specific moiety were generated using the Double Emulsion Solvent Evaporation (DESE) and Single Emulsion Solvent Evaporation (SESE) procedures [61, 62]. In the current investigation, Soluplus was used as a surfactant or polymeric stabiliser. The following characteristics of each synthesised nanoparticle were assessed: drug loading, entrapment efficiency, zeta-potential, and particle size. Since the nanoparticles made with Soluplus as a stabiliser yielded the anticipated outcomes, Scanning Electron Microscopy (SEM) was used to analyse the

surface morphology. In order to investigate the in vitro cytotoxicity effect of PLGA NPs, 3-(4, 5-dimethylthiazol-2-yl)-2, 5-diphenyl tetrazolium bromide (MTT, Sigma) was reduced to Formazan using a breast cancer cell line, including MCF7 [63]. The potential cytotoxicity of synthesised blank PLGA-NPs was also examined. These were employed as a control sample. On MCF7 cells, the in vitro cytotoxicity of free medicine and PLGA-PEG was also assessed. The findings demonstrated that PLGA-NPs exhibited more cytotoxicity than the drug in its unbound state. The cellular absorption of FITC-labelled PLGA-NPs was evaluated by fluorescence imaging microscopy to determine whether the Resveratrol-encapsulated NPs were internalised by the breast cancer cell line MCF7. FITC-labeled PLGA-NPs had a significantly ( $p < 0.05$ ) higher absorption rate than the control. Fluorescence imaging microscopy results demonstrated the successful internalisation of FITC-labeled PLGA-NPs into MCF7 cells. In summary, the present study demonstrated the successful fabrication of PLGA nanoparticles containing resveratrol and the considerable enhancement of the drug's cytotoxicity and distribution by formulation. The investigation also demonstrated the potential surfactant efficacy of soluplus® in the synthesis of nanoparticles. However, there are many limitations to this work, one of which is the lack of an in vivo study to validate the in vitro findings. In addition, the MTT cytotoxicity experiment might have included a normal cell line to offer a contrast that would have bolstered the study's findings. Future studies could be carried out to produce more PLGA nanoparticles and evaluate them more thoroughly utilizing animal models.

## CONCLUSION

In this study, PLGA nanoparticles containing Resveratrol were produced using single and double emulsion-solvent evaporation techniques, with Soluplus® acting as a stabilising agent. The formulation (SF2) was chosen as the best formulation based on its characterisation. Its morphological characteristics were examined with a Scanning Electron Microscope (SEM). SEM images revealed polymeric nanoparticles in the shape of spheres. Following a 48-hour testing period, the lyophilized polymeric nanoparticles of formulation SF2 loaded with Resveratrol released a greater amount of medication than the other formulations. The findings of the pharmacokinetic modelling showed that the matrix type nanoparticle formulation's drug release exponent (n-value) was less than 0.5, suggesting a "Fickian diffusion" of the drug (SF2). In the current study, PLGA nanoparticles containing resveratrol were successfully generated and evaluated by the use of Soluplus® as a surfactant. The effectiveness of Soluplus® as a surfactant and drug-loaded nanoparticle delivery system with the right drug loading, shape, and particle size has been shown by this work. In conclusion, PLGA nanoparticles loaded with resveratrol are efficient and promising delivery systems for anticancer drugs.

## CONFLICT OF INTEREST

Conflict of interest declared none.

REFERENCES

1. Horvath P, Barrangou R. CRISPR/Cas, the immune system of bacteria and archaea. *Sci*. 2010;327:167-170.
2. Long C, McAnally JR, Shelton JM, Mireault AA, Bassel-Duby R, Olson EN. Prevention of muscular dystrophy in mice by CRISPR/Cas9-mediated editing of germline DNA. *Sci*. 2014;345:1184-1188.
3. Xue W, Chen S, Yin H, Tammela T, Papagiannakopoulos T, et al. CRISPR-mediated direct mutation of cancer genes in the mouse liver. *Nat*. 2014;514:380-384.
4. Yin H, Xue W, Chen S, Bogorad RL, Benedetti E, et al. Genome editing with Cas9 in adult mice corrects a disease mutation and phenotype. *Nat Biotechnol*. 2014;32:551-553.
5. Murakami T, Sunada Y. Plasmid DNA gene therapy by electroporation: principles and recent advances. *Curr Gene Ther*. 2011;11:447-456.
6. Zolochovska O, Xia X, Williams BJ, Ramsay A, Li S, et al. Sonoporation delivery of interleukin-27 gene therapy efficiently reduces prostate tumor cell growth in vivo. *Hum Gene Ther*. 2011;22:1537-1550.
7. Maggio I, Holkers M, Liu J, Janssen JM, Chen X, et al. Adenoviral vector delivery of RNA-guided CRISPR/Cas9 nuclease complexes induces targeted mutagenesis in a diverse array of human cells. *Sci Rep*. 2014;4:5105.
8. Ehrke-Schulz E, Schiwon M, Leitner T, Dávid S, Bergmann T, et al. CRISPR/Cas9 delivery with one single adenoviral vector devoid of all viral genes. *Sci Rep*. 2017;7:17113.
9. Cohen H, Levy RJ, Gao J, Fishbein I, Kousaev V, et al. Sustained delivery and expression of DNA encapsulated in polymeric nanoparticles. *Gene Ther*. 2000;7:1896-1905.
10. Acharya S, Sahoo SK. PLGA nanoparticles containing various anticancer agents and tumour delivery by EPR effect. *Adv Drug Deliv Rev*. 2011;63:170-183.
11. Danhier F, Ansorena E, Silva JM, Coco R, Le Breton A, et al. PLGA-based nanoparticles: an overview of biomedical applications. *J Control Release*. 2012;161:505-522.
12. Ke F, Luu YK, Hadjiargyrou M, Liang D. Characterizing DNA condensation and conformational changes in organic solvents. *Plos One*. 2010;5:13308.
13. Vance TM, Su J, Fontham ET, Koo SI, Chun OK. Dietary antioxidants and prostate cancer: a review. *Nutr Cancer*. 2013;65:793-801.
14. Eyo E, Tanriverdi Z, Karakus F, Yilmaz K, Unuvar S. Synergistic anti-proliferative effects of cucurbitacin I and irinotecan on human colorectal cancer cell lines. *Clin Exp Pharmacol*. 2016;6:1-6.
15. Yoo HS, Park TG. Folate-receptor-targeted delivery of doxorubicin nanoaggregates stabilized by doxorubicin-PEG-folate conjugate. *J Control Release*. 2004;100:247-256.
16. Sahin K, Cross B, Sahin N, Ciccone K, Suleiman S, et al. Lycopene in the prevention of renal cell cancer in the TSC2 mutant Eker rat model. *Arch Biochem Biophys*. 2015;572:36-39.
17. Trejo-Solis C, Pedraza-Chaverri J, Torres-Ramos M, Jiménez-Farfán D, Cruz Salgado A, et al. Multiple molecular and cellular mechanisms of action of lycopene in cancer inhibition. *Evid Based Complement Altern Med*. 2013; 1-17.
18. Teodoro AJ, Oliveira FL, Martins NB, Maia GD, Martucci RB, et al. Effect of lycopene on cell viability and cell cycle progression in human cancer cell lines. *Cancer cell int*. 2012;12:1-9.
19. Wang Z, Fan J, Wang J, Li Y, Xiao L, et al. Protective effect of lycopene on high-fat diet-induced cognitive impairment in rats. *Neurosci Lett*. 2016;627:185-191.
20. Alvi SS, Ansari IA, Khan I, Iqbal J, Khan MS. Potential role of lycopene in targeting proprotein convertase subtilisin/kexin type-9 to combat hypercholesterolemia. *Free Radic Biol Med*. 2017;108:394-403.
21. Tvrdá E, Kováčik A, Tušimová E, Paál D, Mackovitch A, et al. Antioxidant efficiency of lycopene on oxidative stress-induced damage in bovine spermatozoa. *J Anim Sci Biotechnol*. 2016;7:1-3.
22. Yang PM, Wu ZZ, Zhang YQ, Wung BS. Lycopene inhibits ICAM-1 expression and NF-κB activation by Nrf2-regulated cell redox state in human retinal pigment epithelial cells. *Life Sci*. 2016;155:94-101.
23. Lee LK, Foo KY. An appraisal of the therapeutic value of lycopene for the chemoprevention of prostate cancer. *Nutr Approach Food Res Int*. 2013;54:1217-1228.
24. Rock EM, Parker LA. Cannabinoids as potential treatment for chemotherapy-induced nausea and vomiting. *Front Pharmacol*. 2016;7:1-10.
25. Betancourt T, Brown B, Brannon-Peppas L. Doxorubicin-loaded PLGA nanoparticles by nanoprecipitation: preparation, characterization and in vitro evaluation. 2007; 2.
26. Yadav K, Yadav D, Yadav M, Kumar S. Noscaphine loaded PLGA nanoparticles prepared using oil-in-water emulsion solvent evaporation method. *J Nanopharm Drug Deliv*. 2016;3:97-105.
27. McCall RL, Sirianni RW. PLGA nanoparticles formed by single-or double-emulsion with vitamin E-TPGS. *JOVE*. 2013; 27.
28. Dian L, Yu E, Chen X, Wen X, Zhang Z, et al. Enhancing oral bioavailability of quercetin using novel soluplus polymeric micelles. *Nanoscale Res Lett*. 2014;9:1-11.
29. Jog R, Kumar S, Shen J, Jugade N, Tan DC, et al. Formulation design and evaluation of amorphous ABT-102 nanoparticles. *Int J Pharm*. 2016;498:153-169.
30. Ling Y, Huang Y. Preparation and release efficiency of poly (lactic-co-glycolic) acid nanoparticles for drug loaded paclitaxel. In 7th: APCMBE China. 2008;19:514-517.
31. Gupta A, Kaur CD, Saraf S, Saraf S. Formulation, characterization, and evaluation of ligand-conjugated biodegradable quercetin nanoparticles for active targeting. *Artif Cells Nanomed Biotechnol*. 2016;44:960-970.
32. Shen J, Burgess DJ. In vitro dissolution testing strategies for nanoparticulate drug delivery systems: recent developments and challenges. *Drug Deliv Transl Res*. 2013;3:409-415.
33. D'Souza S. A review of in vitro drug release test methods for nano-sized dosage forms. *Adv Pharm*. 2014;2014:1-2.
34. Ahmed S, Kaur K. Design, synthesis, and validation of an in vitro platform peptide-whole cell screening assay using MTT reagent. *J Taibah Univ Sci*. 2017;11:487-496.
35. Angius F, Floris A. Liposomes and MTT cell viability assay: an incompatible affair. *Toxicol In Vitro*. 2015;29:314-319.
36. Eren Y, Öztaç A. Determination of mutagenic and cytotoxic effects of Limonium globuliferum aqueous extracts by Allium, Ames, and MTT tests. *Rev Bras Farmacogn*. 2014;24:51-59.
37. Lupu AR, Popescu T. The noncellular reduction of MTT tetrazolium salt by TiO2 nanoparticles and its implications for cytotoxicity assays. *Toxicol Vitro*. 2013;27:1445-1450.
38. Chawla JS, Amiji MM. Biodegradable poly (ε-caprolactone) nanoparticles for tumor-targeted delivery of tamoxifen. *Int J Pharm*. 2002;249:127-138.
39. Chawla JS, Amiji MM. Cellular uptake and concentrations of tamoxifen upon administration in poly (ε-caprolactone) nanoparticles. *Aaps Pharmsci*. 2003;5:28-34.
40. Esmaeili F, Ghahremani MH, Ostad SN, Atyabi F, Seyedabadi M, et al. Folate-receptor-targeted delivery of docetaxel nanoparticles prepared by PLGA-PEG-folate conjugate. *J Drug Target*. 2008;16:415-423.
41. Kapp T, Francke P, Gust R. Investigations on Surface Modified Dendrimers: Enzymatic Hydrolysis and Uptake into MCF-7 Breast Cancer Cells. *Chem Enabling Drug Discov*. 2008;3:635-641.
42. Sahoo SK, Labhasetwar V. Enhanced antiproliferative activity of transferrin-conjugated paclitaxel-loaded nanoparticles is mediated via sustained intracellular drug retention. *Mol Pharm*. 2005;2:373-383.
43. Yi Y, Kim JH, Kang HW, Oh HS, Kim SW, et al. A polymeric nanoparticle consisting of mPEG-PLA-Toco and PLMA-COONa as a drug carrier: improvements in cellular uptake and biodistribution. *Pharm Res*. 2005;22:200-208.
44. MR M, Danaei M, Javanmard R, Raji M, et al. Nanoscale Lipidic Carrier Systems: Importance of Preparation Method and Solvents. *Glob J Nanomed*. 2017;2:1-4.
45. Bulbake U, Doppalapudi S, Kommineni N, Khan W. Liposomal formulations in clinical use: an updated review. *Pceutics*. 2017;9:12.
46. Xu R. Progress in nanoparticles characterization: Sizing and zeta potential measurement. *Particuology*. 2008;6:112-115.
47. Honary S, Zahir F. Effect of process factors on the properties of doxycycline nanovesicles. *Trop J Pharm Res*. 2012;11:169-175.
48. Maji R, Dey NS, Satapathy BS, Mukherjee B, Mondal S. Preparation and characterization of Tamoxifen citrate loaded nanoparticles for breast cancer therapy. *Int J Nanomed*. 2014;25:3107-3118.
49. Alvi M, Yaqoob A, Rehman K, Shoaib SM, Akash MS. PLGA-based nanoparticles for the treatment of cancer: current strategies and perspectives. *AAPS Open*. 2022;8:12.
50. Rezvantala S, Drude NI, Moraveji MK, Güvener N, Koons EK, et al. PLGA-based nanoparticles in cancer treatment. *Front pharmacol*. 2018;9:1260.
51. Cappellano G, Comi C, Chiocchetti A, Dianzani U. Exploiting PLGA-based biocompatible nanoparticles for next-generation tolerogenic vaccines against autoimmune disease. *Int J Mol Sci*. 2019;20:204.
52. Zielińska A, Carreiró F, Oliveira AM, Neves A, Pires B, et al. Polymeric nanoparticles: production, characterization, toxicology and ecotoxicology. *Mol*. 2020;25:3731.
53. Singh R, Lillard Jr JW. Nanoparticle-based targeted drug delivery. *Exp Mol Pathol*. 2009;86:215-223.
54. Tabatabaei Mirakabad FS, Nejati-Koshki K, Akbarzadeh A, Yamchi MR, et al. PLGA-based nanoparticles as cancer drug delivery systems. *Asian Pac J Cancer Prev*. 2014;15:517-535.
55. Gu P, Wusiman A, Wang S, Zhang Y, Liu Z, et al. Polyethylenimine-coated PLGA nanoparticles-encapsulated Angelica sinensis polysaccharide as an adjuvant to enhance immune responses. *Carbohydr Polym*. 2019;223:115-128.
56. Maksimenko O, Malinovskaya J, Shipulo E, Osipova N, Razzhivina V, et al. Doxorubicin-loaded PLGA nanoparticles for the chemotherapy of glioblastoma: Towards the pharmaceutical development. *Int J Pharm*. 2019;572:118733.
57. Todaro B, Moscardini A, Luin S. Pioglitazone-loaded PLGA nanoparticles: towards the most reliable synthesis method. *Int J Mol Sci*. 2022;23:1-20.
58. Sun L, Xu H, Xu JH, Wang SN, Wang J W, et al. Enhanced antitumor efficacy of curcumin-loaded PLGA nanoparticles coated with unique fungal hydrophobin. *AAPS Pharm Sci Tech*. 2020;21:1.
59. Andima M, Costabile G, Isert L, Ndakala AJ, Derese S, et al. Evaluation of β-Sitosterol loaded PLGA and PEG-PLA nanoparticles for effective treatment of breast cancer: Preparation, physicochemical characterization, and antitumor activity. *Pceutics*. 2018;10:232.
60. Alshetali AS. Gefitinib loaded PLGA and chitosan coated PLGA nanoparticles with magnified cytotoxicity against A549 lung cancer cell lines. *Saudi J Biol Sci*. 2021;28:5065-5073.

---

<p>61. Ghasemian E, Vatanara A, Rouholamini Najafabadi A, Rouini MR, Gilani K, et al. Preparation, characterization and optimization of sildenafil citrate loaded PLGA nanoparticles by statistical factorial design. <i>DARU J Pharm Sci.</i> 2013;21:1-10.</p> <p>62. Nabi-Meibodi M, Vatanara A, Najafabadi AR, Rouini MR, Ramezani V, et al. The effective encapsulation of a hydrophobic lipid-insoluble drug in</p>	<p>solid lipid nanoparticles using a modified double emulsion solvent evaporation method. <i>Colloids Surf B Biointerfaces.</i> 2013;112:408-414.</p> <p>63. Kumar P, Nagarajan A, Uchil PD. Analysis of cell viability by the MTT assay. <i>Cold Spring Harb Protoc.</i> 2018.</p>
---	---

---